European Journal of Chemistry

Journal webpage: www.eurjchem.com

Synthesis, spectral characterization, thermal analysis and DFT computational studies of 2-(1*H*-indole-3-yl)-5-methyl-1*H*-benzimidazole and their Cu(II), Zn(II) and Cd(II) complexes

Jabbar Saleh Hadi [1,*], Zuhir Ali Abdulnabi [2] and Adil Muala Dhumad [1]

[1] *College of Education for Pure Science, Basrah University, Basrah, 61004, Iraq*
[2] *Marine Science Center, Basrah University, Basrah, 61004, Iraq*

** Corresponding author at: College of Education for Pure Science, Basrah University, Basrah, 61004, Iraq.*
Tel.: +964.771.0822193. Fax: +964.771.0822193. E-mail address: jshalkabi2@gmail.com (J.S. Hadi).

ARTICLE INFORMATION

DOI: 10.5155/eurjchem.8.3.252-257.1598

Received: 09 June 2017
Received in revised form: 02 July 2017
Accepted: 23 July 2017
Published online: 30 September 2017
Printed: 30 September 2017

KEYWORDS

Metal complex
Benzamidazole
Indol carboxaldehyde
HOMO-LUMO energies
Coats-Redfern method
Density function theory

ABSTRACT

Cu(II), Zn(II) and Cd(II) metal complexes were obtained by using ligand (2-(1*H*-indol-3-yl)-5-methyl-1*H*-benzo[*d*]imidazole) derived from 4-methyl-1,2-phenelyenediamine and indole-3-carboxaldehyde. The ligand and its metal complexes were characterized by elemental analysis, Mass Spectrometry, FT-IR, ^{1}H NMR, ^{13}C NMR, TG and molar conductance measurements. The non-electrolytic behaviour of complexes is confirmed by low molar conductance value. The presence of lattice and coordinated water molecules is confirmed by thermal analysis. Thermodynamic parameters (E, ΔH, ΔS and ΔG) were calculated by using Coats-Redfern method. The density function theory (DFT) calculation at the B3LYP/LanL2DZ method with 6-311+G(d,p) basis set are used to investigate the electronic structure of the ligand and their complexes with Cu(II), Zn(II) and Cd(II) metals. HOMO-LUMO energies of the mentioned compounds have been computed by using DFT/B3LYP calculation method with 6-311+G(d,p) basis set and LanL2DZ basis set for Cu(II), Zn(II) and Cd(II) metal complexes. Mulliken charge distributions of the investigated compounds were also computed with same level of method.

Cite this: *Eur. J. Chem.* **2017**, *8(3)*, 252-257

1. Introduction

The benzimidazole is as a class of heterocyclic compound, consisting of a benzene ring fused to an imidazole ring [1-3]. There are different methods of preparing them using various reagents such as, carboxylic acid, esters, amides, aldehydes etc., when reacted with *o*-phenylenediamine and their derivatives, afforded the benzimidazoles. Methods of benzimidazoles synthesis from the condensation of 1,2-phenylenediamine with aromatic aldehydes under oxidative condition are simple and efficient method and the reactions give high yields in short time and easy in isolation. The reaction carried out in air under reflux or in room temperature in presence an oxative reagent such as H_2O_2 [3], $Pb(OAC)_2$ [4], or in presence a catalyst such as cupric acetate [5]. The complexes of transition metals with benzimidazole have been extensively studied due to the ability of benzimidazoles as excellent *N*-donor ligands [6]. Most of benzimidazoles possess antibacterial, fungicide, antihelmintic and antitumor activity [7]. The numbering system for benzimidazoles is given in Scheme 1 [3]. Substitution at 2 position of benzimidazole ring is very important for their pharmacological effect [8].

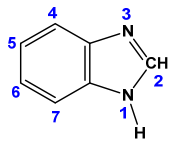

Scheme 1

2. Experimental

2.1. Apparatus

FT-IR spectra were recorded in the range 4000-500 cm^{-1} using KBr disc on Shimadzu FT-IR 8400S spectrometer. ^{1}Hand ^{13}C NMR spectra were recorded on Bruker 400 spectrometer (400 MHz for ^{1}H NMR and 100 MHz for ^{13}C NMR) using DMSO-d_6 as a solvent and TMS as an internal reference. Mass spectrum for the ligand was recorded on Agilent Technologies-5975C (EI, 70 eV). The thermal analyses (TG and DTG) were carried out in dynamic nitrogen atmosphere (20 mL/min) with a heating rate of 10 °C/min using a Perkin-Elmer thermal analyzer.

ISSN 2153-2249 (Print) / ISSN 2153-2257 (Online)
http://dx.doi.org/10.5155/eurjchem.8.3.252-257.1598

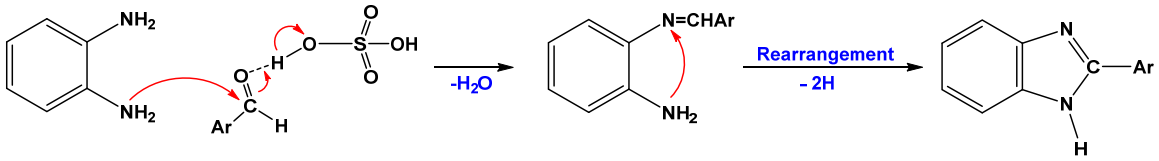

Scheme 2

The TLC type silica gel $60F_{254}$ was used to monitor the reaction and the spots were visualized by UV lamp Black-Ray-B-100A. Molar conductance of the freshly prepared solutions (1×10^{-3} M in DMSO) was measured at room temperature using W.T.W-Conductivity meter. The metal content of the prepared complex was found by a Buck 210 BGP model atomic absorption spectrometer after digestion in nitric acid. Elemental analyses for C, H and N were performed using a Leco CHNS-932 Analyzer.

2.2. Materials and methods

2.2.1. Material

4-Methyl-1,2-phenelyenediamine from Merck and used after recrystallization from hexane. Indol-3-carboxaldehyde from Himedia and used as supplied various metal (II) acetate were of Fluka, all other solvents are of analytical grade.

2.2.2. Synthesis

2.2.2.1. Synthesis of ligand, 2-(1H-indol-3-yl)-5-methyl-1H-benzo[d]imidazole

An ethanolic solution (15 mL) of 5 mmole (0.725 g) of indole-3-carboxaldehyde and ethanolic solution (10 mL) of 5 mmole (0.61 g) of 4-methyl-1,2-phenelyene diamine mixed and refluxed in presence of 2 drops of concentrated sulphuric acid [2] for 2h with continuous stirring. The orange precipitate which separated filtered hot and washed with hot ethanol and then with ether several times and dried at 70 °C in oven. The crude product was recrystallized from DMF:H_2O (1:10, *v*:*v*). Color: Reddish orange. Yield: 70%. M.p.: 235-237 °C. FT-IR (KBr, ν, cm^{-1}): 3400 (N-H, Benz.), 3128 (N-H, Indole), 3047 (Ar-H), 2920, 2866 (CH_3), 1633 (C=N). ^{1}H NMR (400 MHz, DMSO-d_6, δ, ppm): 2.30 (s, 3H, CH_3), 7.05-8.33 (m, 8H, Ar-H), 11.00 (s, 1H, NH-indole), 11.86 (s, 1H, NH-imidazole). ^{13}C NMR (100 MHz, DMSO-d_6, δ, ppm): 149.50 (C_{16}), 136.29 (C_2), 135.99 (C_{10}), 133.71 (C_{14}), 130.22 (C_{11}), 126.16 (C_3), 125.98 (C_7), 125.51 (C_{13}), 122.22 (C_6), 121.31 (C_4), 120.13 (C_5), 118.74 (C_9), 118.18 (C_{12}), 111.62 (C_1), 105.22 (C_8), 21.19 (C_{15}). MS (EI, *m/z* (%)): 247.2 (M^+, 100). Anal. calcd. for $C_{16}H_{13}N_3$: C, 77.71; H, 5.30; N, 16.99. Found: C, 77.63; H, 5.44; N, 17.04 %.

2.2.2.2. Synthesis of [Cu(L)H_2O.CH_3COO].H_2O (LCu)

Ethanolic solution (20 mL) of 1 mmole (0.247 g) of ligand was add to a hot ethanolic solution (20 mL) of $Cu(CH_3COO)_2$ (0.199 g). The resulting mixture color change immediately to black and then refluxing for 3 h., the precipitate was filtered and washed with hot ethanol several time, then dried to afford green powder. Color: Green. Yield: 72%. M.p.: > 300 °C. FT-IR (KBr, ν, cm^{-1}): 3400 (N-H, Benz.), 1616 (C=N). Anal. calcd. for $C_{18}H_{19}N_3O_4Cu$: C, 53.39, H, 4.73, N, 10.38, Cu, 15.69. Found: C, 51.97; H, 4.87; N, 10.69; Cu, 16.43%. Λ_m(S.m^2.mol^{-1}): 6.1.

2.2.2.3. Synthesis of [Zn(L)H_2O.CH_3COO] (LZn)

Ethanolic solution of 1 mmole (20 mL) of ligand and a hot ethanolic solution of 1 mmole $Zn(CH_3COO)_2$ (0.219 g) was refluxed for 6 h, the precipitate was filtered and washed with hot ethanol several time. The brown precipitate was collected and dried. Color: Brown. Yield: 45%. M.p.: >300 °C. FT-IR (KBr, ν, cm^{-1}): 3400 (NH, Benzimidazole), 1627 (C=N). Anal. calcd. for $C_{18}H_{21}N_3O_5Zn$: C, 50.90; H, 4.98; N, 9.89; Zn, 15.39. Found: C, 49.47; H, 5.13; N, 10.18; Zn, 16.07%. Λ_m (S.m^2.mol^{-1}): 3.2. ^{1}H NMR (400 MHz, DMSO-d_6, δ, ppm): 11.63 (s, 1H, NH-benzimidazole), 8.72-6.97 (m, 8H, Ar-H), 2.35 (s, 3H, CH_3).

2.2.2.4. Synthesis of [Cd(L)H_2O.CH_3COO] (LCd)

Ethanolic solution of 1 mmole of ligand and a hot ethanolic solution of $Cd(CH_3COO)_2$ 1 mmole (0.266 g) was refluxed for 4 h and the mixture filtered hot, the precipitate washed with hot ethanol and the obtained solid dried. Color: Brown. Yield: 37%. M.p.: > 300 °C. FT-IR (KBr, ν, cm^{-1}): 3400 (NH, benzimi-dazole), 1621 (C=N). Anal. calcd. for $C_{18}H_{19}N_3O_4Cd$: C, 47.64; H, 4.22; N, 9.26;Cd, 24.77. Found: C, 46.22; H, 4.34; N, 9.51; Cd, 24.81%. Λ_m (S.m^2.mol^{-1}): 4.6.

2.2.3. Computational details

All computations were performed using the Gaussian09 software package [9]. Full geometry optimizations were carried out using the Density Function Theory at B3LYPlevel for studied ligand and their Cd(II), Cu(II) and Zn(II) complexes [10,11]. LANL2DZ is a basis set for post-third-row atoms which uses effective core potentials in order to reduce computational cost [12]. Properties and HOMO-LUMO energies of the ligand and their complexes was calculated by the LanL2DZ basis set for the Cd, Cu and Zn atoms and the 6-311+G(d,p) higher basis set level for N, O, C and H atoms. Mulliken charge distributions of the investigated compounds were also computed at same level of method.

3. Results and discussion

3.1. Characterization of ligand

The benzimidazole ligand, 2-(1*H*-Indol-3-yl)-5-methyl-1*H*-benzo[*d*]imidazole, was formed according to the mechanism of Scheme 2. The ligand insoluble in hexane, benzene, toluene, diethyl ether and chloroform; sparingly soluble in methanol and ethanol and very soluble in DMSO and DMF. The ligand exhibits two bands for νN-H the first is a strong and a broad at 3400 cm^{-1} attributed to νN-H of benzimidazole moiety [13,14], the second at 3128 cm^{-1} weak and broad attributed to νN-H of indole moiety. The weak band at 3047 cm^{-1} attributed to νC-H aromatic and the bands at 2920 and 2866 cm^{-1} attributed to νC-H asym and sym stretching of CH_3 group. The strong band at 1633 cm^{-1} attributed to νC=N stretching mode.

The mass spectrum confirms the proposed formula where the molecular ion peak (100%) at 247.2 *m/z*, which is fit the molecular weight and the high relative abundance gives an idea of the stability of molecular ion (Figure 1).

The ^{1}H NMR spectrum of ligand shows a signal at δ 11.86 ppm attributed to NH proton of benzimidazole moiety [14,15], another single signal at δ 11.00 ppm attributed to NH proton of indole moiety [16,17].

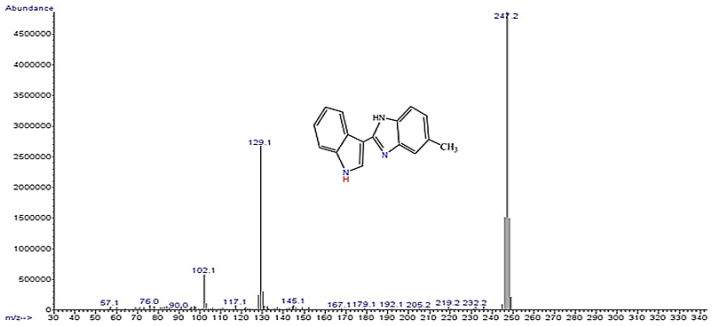

Figure 1. The mass spectrum of ligand.

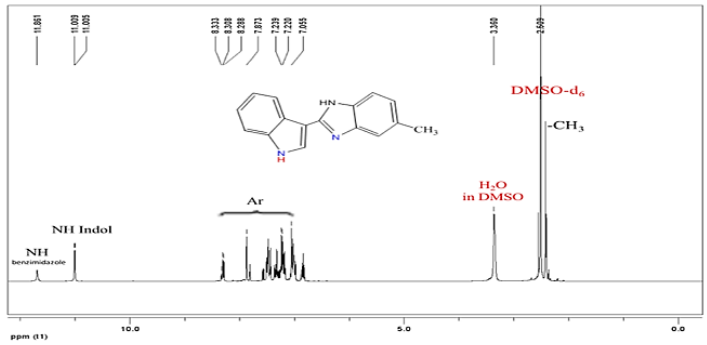

Figure 2. The ^{1}H NMR-d_6 spectrum of ligand.

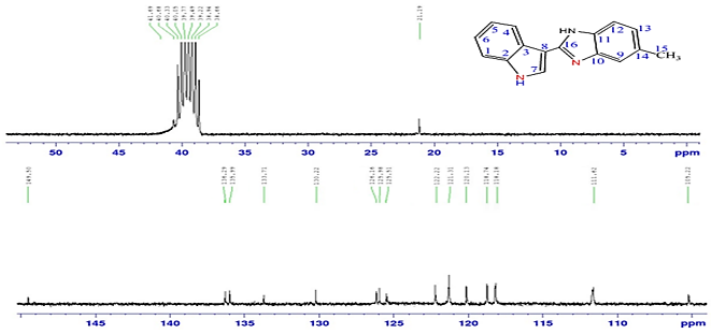

Figure 3. The ^{13}C NMR spectrum of ligand.

The aromatic protons appear in the expected region as multiples signals in the range δ 7.05-8.33 ppm. The methyl protons appear as a singlet signal at δ 2.30 ppm. The ^{1}H NMR spectrum of ligand as shown in Figure 2.

The ^{13}C NMR spectrum shows a signal at δ 21.19 ppm attributed to methyl carbon and a signal at δ 149.5 ppm to C=N (Figure 3) [18]. All signals attributed to aromatic carbon are listed experimental section together with the numbering system of the ligand.

3.2. Characterization of the metal complexes

The Zn(II), Cu(II) and Cd(II) complexes are stable, non-hygroscopic and having high melting points (>300 °C). These complexes are insoluble in common organic solvent but they soluble in DMF and DMSO except Cd(II) complex also insoluble in DMSO.

The elemental analysis CHN and the metal ratio in the complexes are in agreement with suggested formula which indicates that the ligand associates with metal (ions) in 1:1 molar ratio. The molar conductance measurements indicate their non-electrolytic nature.

To elucidation the site of binding between ligand and metal ions, IR spectroscopy gives good evidence when compared the IR spectrum of ligand with IR spectra of complexes, the band at 3400 cm^{-1} which attributed to stretching vibration of N-H (benzimidazole) in free ligand, this remain unchanged in the complexes spectra, indicating that this group in not participating in coordination but the band at 3128 cm^{-1} which attributed to N-H of indol moiety in free ligand is totally disappearance. This data is suggested that the deprotonation and participating through the nitrogen atom of indole. The band at 1633 cm^{-1} which attributed to C=N in free ligand is shifted to a lower wave number side (Δν = 6-17 cm^{-1}) in all complexes indicates the participation of the C=N group in coordination to the metal ions through the lone pair of electrons on the nitrogen atom [17].

The ^{1}H NMR spectrum of Zn complex (diamagnetic) (Figure 4) when compared with the ligand spectrum, shows only the signal of benzamidazole N-H at δ 11.63 ppm which

Table 1. Kinetic parameters of the complexes using the Coats-Redfern equation.

Compound	Step	A (1/s)	*E* (kJ/mol)	Δ*H* (kJ/mol)	Δ*S*(kJ/mol.K)	Δ*G*(kJ/mol)	r^2
[Cu(L)H_2O.CH_3COO].H_2O	1st	1.30789	22.578	19.518	-0.2444	109.469	0.937
	2nd	2.2971×10^{2}	51.707	47.234	-0.2046	157.319	0.945
	3rd	7.15107	44.356	39.468	-0.2342	177.180	0.917
	4th	1.9666×10^{6}	167.409	159.444	-0.1341	287.944	0.944
[Zn(L)H_2O.CH_3COO]	1st	0.14027	16.230	13.129	-0.2631	111.267	0.949
	2nd	1.7367×10^{2}	54.245	49.897	-0.2067	158.006	0.959
	3rd	9.9223×10^{5}	121.619	115.608	-0.1374	221.018	0.977
[Cd(L)H_2O.CH_3COO]	1st	28.4553	31.197	28.096	-0.2189	109.760	0.966
	2nd	1.372×10^{16}	167.475	163.501	0.0600	134.777	0.980
	3rd	5.187×10^{-3}	12.466	7.7436	-0.2940	174.745	0.956
	4th	1.3452×10^{4}	101.746	95.818	-0.1731	219.254	0.949

indicated that this group not participation in complex formation while the signal at δ 11.00 ppm in ligand spectrum which attributed to NH proton (indole moiety) is totally absent in the complex spectrum which indicated the deprotonation of NH group and subsequently the replacement of proton by metal.

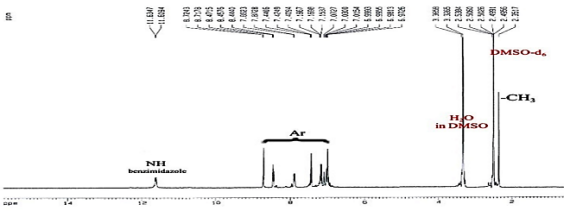

Figure 4. The ^{1}H NMR spectrum of Zn complex.

3.3. Thermal degradation

3.3.1. Thermal degradation of [Cu(L)(H₂O)(CH₃COO)].H₂O

The TG/DTG curve of the [Cu(L)(H_2O)(CH_3COO)].H_2O shows the four steps decomposition. The first step in the range 50-125 °C (DTG_{max} = 95 °C) with mass loss 4.93% (theoretical 4.45%) which indicates the presence of one lattice water molecule. The second step with mass loss 4.89% (theoretical 4.66%) which attributed to one coordinated water molecule [19]. The third and fourth steps take place in fast rate (Figure 5) starting from 275 °C to the final temperature 800 °C. The residual part 28%, may be attributed to the CuO polluted with carbon [19,20].

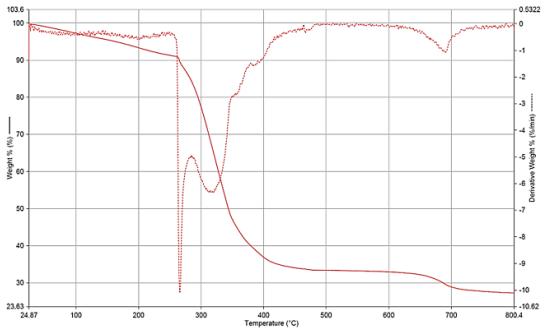

Figure 5. TG/DTG curve of copper complex.

3.3.2. Thermal degradation of [Zn(L)(H₂O)(CH₃COO)].2H₂O

The TG/DTG curve of the zinc complex shows three steps of degradation, the first step 8.49% (theoretical 8.49%) weight loss in the range 50-169 °C corresponds to two lattice water molecules [20]. The second step in the range 185-345 °C with mass loss 20.2% (theoretical 20.1%) which represent the loss of both acetate and coordinated water together. The last step begin at 350 °C and end at 600 °C to afford the final degradation of ligand and the final product is ZnO 19.72% (theoretical 19%) [19,20].

3.3.3. Thermal degradation of [Cd(L)(H₂O)(CH₃COO)].H₂O

The TG/DTG curve of the cadmium complex shows four steps decomposition and similar to the Cu complex, where the first step 50-150 °C (DTG_{max} = 100 °C) with mass loss 3.83% (theoretical 3.97%) which indicated the presence of one lattice water molecule [20]. The second and third steps in the range 170-410 °C with total mass loss 17.77% (theoretical 17.93%) equivalent to one coordinated water molecule and acetate. The fourth step starting from 415 to 800 °C and the final residue 27.85% (theoretical 28.25%) which indicated that the final product is cadmium (II) oxide.

3.4. Kinetic and thermodynamic analysis

The thermal dehydration and decomposition of the complexes were studied using Coats-Redfern method [20,21].

$$\log\left[\frac{\log\frac{Wf}{Wf-Wt}}{T^2}\right]=\log\left[\frac{A\times R}{\theta\times E}\left(1-\frac{2\times R\times T}{E}\right)\right]-\frac{E}{2.303\times R\times T} \quad (1)$$

where Wf and Wt are weight at the end step and at any temperature, respectively; *E*, activation energy; R, Gas constant (8.314×10^{-3} kJ/mole); Θ, heating rate and A, pre-exponential factor. The decomposition steps of all complexes show a best fit for first order in all steps. The correlation coefficient (r^2) was computed using the least square method by plotting the left hand side of Coats-Redfern equation versus 1000/T (Figure 6). The activation energy and the exponential factor were calculated from the slope and intercept, respectively. Δ*H*, Δ*S* and Δ*G* for all steps were calculated by using the Equation (2-4).

$$\Delta H = \Delta E - R\times T \quad (2)$$

$$\Delta S = R \times \ln (A\times h/KB\times TS) \quad (3)$$

$$\Delta G = \Delta H - T\times\Delta S \quad (4)$$

whereas, h, Planck constant (6.6262×10^{-34} J.s);K_B, Boltzman constant (1.3806×10^{-23} J/K) and T_S (T_{max} from DTG curve). The thermokinetic data are summarized in Table 1. From this result, the high activation energy for all complexes indicated the high stability of the complexes. In general, the activation energy of the second steps are higher than first step, this indicated that the dehydrated complexes are more stable, in addition the positive value of Δ*H* means that the decomposition process are endothermic. The negative values of Δ*S* indicated that the complexes more ordered than the reactants. All values of Δ*G* are positive which indicate that all steps are non-spontaneous [20].

Table 2. Selected bond lengths and angles for ligand and (Cd, Cu and Zn) complexes from the B3LYP and (B3LYP/LANL2DZ/6-311+G(d,p) basis set) calculations.

Parameters	[Cd(L).H_2O.CH_3COO]		[Cu(L).H_2O.CH_3COO].H_2O		[Zn(L).H_2O.CH_3COO]		L	
	Calc.	Exp.	Calc.	Exp.	Calc.	Exp. [22-24]	Calc.	Exp.
Bond lengths (Å)								
M-N25	2.242	2.226	1.916	1.982	2.023	2.037	-	-
M-N13	3.503	-	4.515	-	3.581	-	-	-
M-O37	2.165	-	1.991	-	2.122	2.111	-	-
M-O32	2.200	-	1.982	-	2.025	-	-	-
N25-C26	1.368	1.365	1.382	1.368	1.368	1.370	1.317	-
N25-C14	1.381	1.367	1.397	1.367	1.389	1.360	1.383	-
N13-C12	1.367	1.325	1.332	1.329	1.371	1.320	1.372	-
C11-C26	1.432	-	1.412	-	1.433	-	1.450	-
C11-C12	1.455	-	1.461	-	1.421	-	1.376	-
C11-C3	1.436	-	1.462	-	1.451	-	1.447	-
Bond angle (°)								
C14-N25-M	146.23	133.60	122.56	131.80	133.13	130.30	-	-
C26-N25-M	104.94	119.20	130.36	117.50	119.06	121.10	-	-
C26-N25-C14	107.30	107.30	107.009	107.10	107.46	107.70	105.60	-

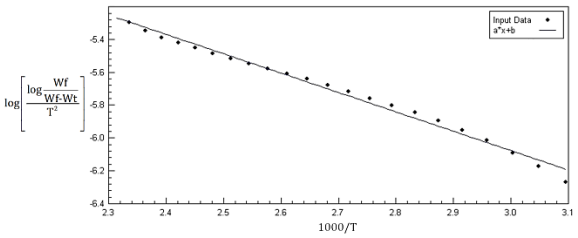

Figure 6. Coats-Redfern [Cu(L)H_2O.CH_3COO].H_2O step1st.

3.5. Computational results

3.5.1. Geometrical optimization

The visualization of the optimized geometrical structure and atomic labeling of [Cd(L)H_2O.CH_3COO] complex calculated by the B3LYP/LanL2DZ method with 6-311+G(d,p) basis set are given in Figure 7.

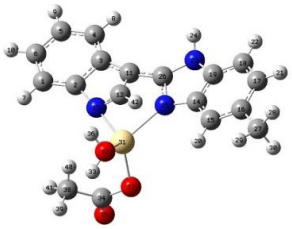

Figure 7. Optimized structures of [Cd(L).H_2O.CH_3COO] complex calculated by the B3LYP/LanL2DZ method with 6-311+G(d,p) basis set with atom numbering.

The optimized geometric parameters are listed in Table 2. The crystallographic structures of 2-(1*H*-indol-3-yl)-5-methyl-1*H*-benzo[*d*]imidazole and their Cu(II), Zn(II) and Cd(II) complexes is not available in the literature, therefore we compared some bond lengths and bond angles with X-ray diffraction data of M-N and N-C as a general. The optimized bond lengths and bond angles of title ligand and complexes are in good agreement with X-ray data [22-24]. N25-C26 in L-Zn complex is shorter and C25-N14 is longer than as expected (1.368 and 1.389 Å, respectively). TheanglesC14-N25-M and C26-N25 were calculated as 146.23° and 104.94° for Cd complex, while the corresponding angles for Cu and Zn complexes are 122.56° and 130.36° and 133.13°, 119.06°, respectively.

3.5.2. Mulliken population analysis

Dipole moment, molecular polarizability and bond properties are affected by atomic charges, therefore, the Mulliken atomic charge calculation has an important role in quantum chemistry [25-27]. Mulliken population analysis was performed using DFT/B3LYP calculation method with 6-311+G(d,p) basis set and LanL2DZ basis set for Cu(II), Zn(II) and Cd(II) metal complexes. Graphical reorientations of Mulliken charge distributions of ligand and L-Cd, L-Cu, L-Zn complexes is shown in Figure 8. As can be seen in Table 3, all the hydrogen atoms have a net positive charge. The obtained atomic charge shows that the Cu atom of [Cu(L)(H_2O)(CH_3COO)].H_2O has lower positive atomic charge (0.494) than the Cd and Zn atoms in the other studied complexes [Cd(L)(H_2O)(CH_3COO)].H_2O and Cd(L)(H_2O)(CH_3COO)].H_2O which obtained 1.032 and 1.033, respectively. The N23 atom has negative atomic charge -0.067, -0.416, -0.428 and -0.439 of ligand, Zn, Cd and Cu complexes, respectively.

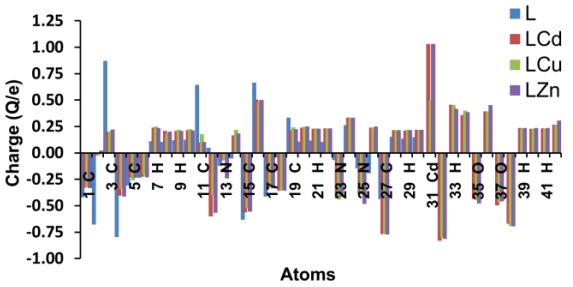

Figure 8. Graphical reorientations of Mulliken charge distributions of ligand L and LCd, LCu, LZn complexes.

3.5.3. Total energies, dipole moments and molecular orbitals analysis

The HOMO energy represents the ability to donate an electron, LUMO energy as an electron acceptor represents the ability to obtain an electron [28]. The HOMO-LUMO energy calculations of the title compounds were performed using DFT/B3LYP method with 6-311+G(d,p) basis set for the ligand and DFT/B3LYP methods with LanL2DZ basis sets for its Cd, Cu and Zn complexes. Furthermore, the orbital shapes (HOMO-LUMO) and the energy gap between the HOMO-LUMO which is a critical parameter to determine molecular electrical transport properties[29] were plotted in 3-dimensional (3D) by using at B3LYP/6-311+G(d,p) and B3LYP/ LanL2DZ levels, respectively, are given in Figure 9. The values of the calculated energies, dipole moment and frontier molecular orbital energies of ligand and Cd, Cu and Zn complexes from the B3LYP and B3LYP/LANL2DZ/6-311+G(d,p) basis set calculations are given in Table 4.

Table 3. The Mulliken atomic charge distribution of ligand L and LCd, LCu, LZn complexes.

Atoms	Mulliken atomic charges (Q/e)				Atoms	Mulliken atomic charges (Q/e)			
	L	LCd	LCu	LZn		L	LCd	LCu	LZn
1 C	-0.418	-0.328	-0.324	-0.333	22 H	0.104	0.232	0.233	0.232
2 C	-0.676	-0.026	-0.020	0.023	23 N	-0.067	-0.428	-0.439	-0.416
3 C	0.872	0.197	0.203	0.224	24 H	0.266	0.333	0.326	0.334
4 C	-0.794	-0.406	-0.339	-0.411	25 N	-0.146	-0.393	-0.393	-0.481
5 C	-0.305	-0.231	-0.258	-0.233	26 C	-0.189	0.238	0.236	0.250
6 C	-0.233	-0.223	-0.211	-0.229	27 C	-0.435	-0.770	-0.767	-0.770
7 H	0.111	0.238	0.251	0.237	28 H	0.155	0.215	0.216	0.214
8 H	0.106	0.207	0.181	0.202	29 H	0.136	0.212	0.218	0.215
9 H	0.122	0.210	0.219	0.209	30 H	0.151	0.218	0.219	0.219
10 H	0.125	0.213	0.225	0.212	31 Cd, Cu, Zn		1.032	0.494	1.033
11 C	0.646	0.098	0.176	0.105	32 O		-0.832	-0.800	-0.814
12 C	0.048	-0.601	-0.404	-0.567	33 H		0.454	0.451	0.418
13 N	-0.120	-0.071	-0.065	-0.241	34 C		0.358	0.400	0.387
14 C	-0.049	0.165	0.217	0.185	35 O		-0.438	-0.446	-0.479
15 C	-0.629	-0.563	-0.524	-0.554	36 H		0.394	0.389	0.451
16 C	0.666	0.503	0.484	0.501	37 O		-0.495	-0.462	-0.459
17 C	-0.412	-0.336	-0.320	-0.336	38 C		-0.669	-0.690	-0.695
18 C	-0.041	-0.355	-0.354	-0.355	39 H		0.235	0.229	0.237
19 C	0.336	0.214	0.243	0.225	40 H		0.229	0.230	0.235
20 H	0.109	0.239	0.248	0.251	41 H		0.231	0.225	0.237
21 H	0.118	0.228	0.231	0.228	42 H		0.267	0.266	0.306

Table 4. Calculated energies, dipole moment and frontier molecular orbital energies of ligand and Cd, Cu and Zn complexes from the B3LYP and B3LYP/LANL2DZ/6-311+G(d,p) basis set calculations.

Compounds	HOMO (eV)	LUMO (eV)	ΔE_{H-L} (eV)	Dipole (Debye)	*E* [RB3LYP] (a.u.)
L	-0.20202	-0.04371	-0.15831	5.1212	-782.006
LCd	-0.19029	-0.06039	-0.12990	6.5635	-1134.090
LCu	-0.19160	-0.05127	-0.14033	5.2374	-1151.646
LZn	-0.20637	-0.04409	-0.16228	5.1698	-1282.169

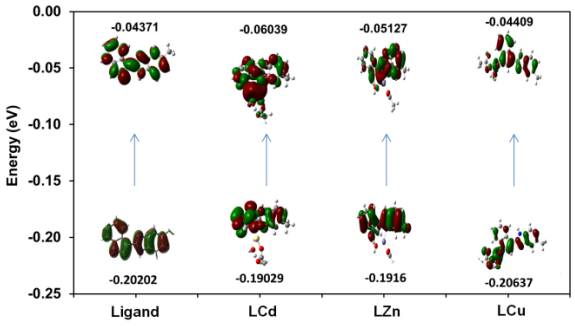

Figure 9. Frontier molecular orbitals and the energy gap between the HOMO-LUMO by using at B3LYP/6-311+G(d,p) and B3LYP/ LanL2DZ levels of ligand L and LCd, LCu, LZn complexes.

The values found for HOMO energy levels are -0.20202, -0.19029, -0.19160 and -0.20637eV of ligand, LCd, LCu and LZn complexes, respectively. The LUMO energy level -0.04371, -0.06039, -0.05127 and -0.04409 eV of ligand, LCd, LCu and LZn complexes, respectively.

References

[1]. Walia, R.; Hedaitullah, M.; Naaz, S. F.; Iqbal, K.; Lamba, H. *Int. J. Res. Pharm. Chem.* **2011**, *1(3)*, 565-574.
[2]. Chawla, A.; Kaur, R.; Goyal, A. *J. Chem. Pharm. Res.* **2011**, *3(6)*, 925-944.
[3]. Meshram, G. A.; Patil, V. D. *Int. J. Chem. Sci.* **2010**, *8(1)*, 119-131.
[4]. Akyuz, G.; Yilmaz, F.; Mentese, E. *Eur. J. Sci. Techn.* **2015**, *2(4)*, 123-127.
[5]. Banjare, S. K.; Payra, S.; Saha, A.; Banerjee, S. *Org. Med. Chem. I. J.* **2017**, *1(4)*, 1-5.
[6]. Podunavac-Kuzmanovic, S.O.; Cvetković,D. M.; Vojinovic,L. S. *Acta Period. Technol.* **2004**, *35*, 239-246.
[7]. Gumus, F.; Algul, O.; Eren, G.; Eroglu H.; Diril N.; Gur S.; Ozkul A. *Eur. J. Med. Chem.* **2003**, *38(5)*, 473-480.
[8]. Karuralam, R. P.; Hands, K. R.; Shetty, S. N. *J. Chil. Chem. Soc.* **2011**, *57(2)*, 1122-1125.
[9]. Frisch, M. J.; Trucks, G. W.; Schlegel, H. B.; Scuseria, G. E.; Robb, M. A.; Cheeseman, J. R.; Scalmani, G.; Barone, V.; Mennucci, B.; Petersson, G. A.; Nakatsuji, H.; Caricato, M.; Li, X.; Hratchian, H. P.; Izmaylov, A. F.; Bloino, J.; Zheng, G.; Sonnenberg, J. L.; Hada, M.; Ehara, M.; Toyota, K.; Fukuda, R.; Hasegawa, J.; Ishida, M.; Nakajima, T.; Honda, Y.; Kitao, O.; Nakai, H.; Vreven, T.; Montgomery, Jr. J. A.; Peralta, J. E.; Ogliaro, F.; Bearpark, M. Heyd, J. J.; Brothers, E.; Kudin, K. N.; Staroverov, V. N.; Kobayashi, R.; Normand, J.; Raghavachari, K.; Rendell, A.; Burant, J. C.; Iyengar, S. S.; Tomasi, J.; Cossi, M.; Rega, N.; Millam, J. M.; Klene, M.; Knox, J. E.; Cross, J. B.; Bakken, V.; Adamo, C.; Jaramillo, J.; Gomperts, R.; Stratmann, R. E.; Yazyev, O.; Austin, A. J.; Cammi, R.; Pomelli, C.; Ochterski, J. W.; Martin, R. L.; Morokuma, K.; Zakrzewski, V. G.; Voth, G. A.; Salvador, P.; Dannenberg, J. J.; Dapprich, S.; Daniels, A. D.; Farkas, O.; Foresman, J. B.; Ortiz, J. V.; Cioslowski, J.; Fox, D. J. (2009) Gaussian 09, Revision A. 1. Gaussian, Inc., Wallingford.
[10]. Becke, A. D. *J. Chem. Phys.* **1993**, *98*, 5648-5652.
[11]. Lee, C.; Yang, W.; Parr, R. G. *Phys. Rev. B* **1988**, *37*, 785-789.
[12]. Karakas, D.; Sayin, K. *Indian J. Chem. A* **2013**, *52*, 480-485.
[13]. Patil, V. D.; Medha, G.; Shramesha, M.;Aarti, J. *Der Chemica Sinica* **2010**, *1(2)*, 125-129.
[14]. Sunitha, M.; Jogl, P.; Ushaiah, B.; Kumari, C. G. *E. J. Chem.* **2012**, *9(4)*,2516-2523.
[15]. Sadek, K. U.; Al-Qalaf, F.; Mekheimer, R. A.; Elnagdi, M. H. *Arab. J. Chem.* **2012**, *5*, 63-66.
[16]. Radha, Y.; Manjula, A.; Reddy, B. M.; Rao, B. V. *Ind. J. Chem. B* **2011**, *50*, 1762-1773.
[17]. Ade, S. B.; Deshpande, M. N.; Kolhatkar, D. G.; Bhagat, S. M. *J. Chem. Pharm. Res.* **2012**, *4(1)*, 105-111.
[18]. Kumar, A.; Kapoor, K. K. *J. Chem. Pharm. Res.* **2011**, *3(6)*, 369-374.
[19]. El-Ajaily, M. M.; El-Ferjani, R. M.; Maihub, A. A. *Jordan J. Chem.* **2007**, *2(3)*, 287-296.
[20]. Ebrahimi, H. P.; Hadi, J. S.; Abdulnabi, Z. A.; Bolandnazar Z. , *Spectrochim. Acta A: Mol. Biomol. Spect.* **2014**, *117*, 485-492.
[21]. Jou, C. S., M. Sc. Thesis, University of Texas Technology, 1986.
[22]. Parajon-Costa, B. S.; Baran, E. J.; Piro, O. E. *Polyhedron* **1997**, *16(19)*, 3379-3383.
[23]. Okabe, N.; Kohyama, Y.; Ikeda, K. *Acta Cryst. C* **1995**, *51*, 222-224.
[24]. Okabe, N.; Ikeda, K.; Kohyama, Y.; Sasaki, Y. *Acta Cryst. C* **1995**, *51*, 224-226.
[25]. Ebrahimi, H. P; Hadi, J. S.; Alsalim, T. A.; Ghali, T. S.; Bolandnazar, Z. *Spectrochim. Acta A: Mol. Biomol. Spect.* **2015**, *137*, 1067-1077.
[26]. Ebrahimi, H. P; Hadi J. S; Al-Ansari, H. S. *J. Mol. Struc.* **2013**, *1039*, 37-45.
[27]. Khodam, H. M.; Hadipour, N. L. *Comp. Theor. Chem.* **2016**, *1098*, 63-69.
[28]. Sahebalzmani, H.; Khaligh, N.; Ghammamy, S.; Salimi, F.; Mehrani, K. *Molecules* **2011**, *16*, 7715-7724.
[29]. Baldenebro-Lopez, J. *Int. J. Mol. Sci.* **2012**, *13*, 16005-16019.

Graphical Abstract

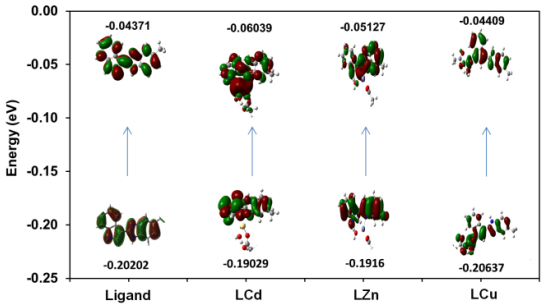

It is very important to confirm the author(s) last, middle and first names in order to be displayed correctly on our website as well as in the indexing databases.

Order of the names must be

First name, Middle name, Last name

Jabbar Saleh Hadi

e-mail: jshalkabi2@gmail.com

Zuhir Ali Abdulnabi

e-mail: zuhir38@yahoo.com

Adil Muala Dhumad

e-mail: adilmuala2013@yahoo.com